Electrical Engineering (2019) 101:1163–1175
https://doi.org/10.1007/s00202-019-00846-1

ORIGINAL PAPER

Transient analysis with coupled field-circuit model and experimental assessment of a PMSG used in small-scale wind turbine for water heating purpose

Yucel Cetinceviz[1] · Erdal Sehirli[1] · Durmus Uygun[2] · Cemil Ocak[3] · Huseyin Demirel[4]

Received: 31 May 2019 / Accepted: 26 September 2019 / Published online: 22 October 2019

Abstract
This paper introduces the detailed coupled field-circuit analysis including performance characteristics of a 4-kW in-running rotor permanent magnet synchronous generator (PMSG) used in rural-type small-scale wind turbines for water heating purpose. The content of the work consists of design, analysis, optimization, production and testing processes and validation studies. An integrated 2D electromagnetic field and circuit model are used in the design and analysis processes. The electrical machine design involves complex and time-consuming processes. This model provides comprehensive information on machine behavior under different conditions and is an effective to demonstrate compliance with real load conditions prior to the manufacture. The goal of the optimization process is to find a design that offers cost, manufacturability and efficiency as well as generator output values. For this, a multiobjective optimization approach has been used. Typical design and simulation principles are applied to the designed PMSG, respectively, including calculation and evaluation of various output parameters for different simulated wind speed rates and varying load conditions. Furthermore, the analytical studies related to finite element methods and parametric approaches are presented in collaboration with experimental studies carried out for different load rates.

Keywords Coupled circuit model · Permanent magnet synchronous generator · Prototype · Finite element method

✉ Yucel Cetinceviz
ycetinceviz@kastamonu.edu.tr

Erdal Sehirli
esehirli@kastamonu.edu.tr

Durmus Uygun
durmus.uygun@aegeandynamics.com

Cemil Ocak
cemilocak@gazi.edu.tr

Huseyin Demirel
hdemirel@karabuk.edu.tr

[1] Electrical and Electronics Engineering Department, Kastamonu University, Kuzeykent Mahallesi Org. Atilla Ates Pasa Caddesi, 37150 Merkez, Kastamonu, Turkey

[2] Aegean Dynamics Inc. Co., Ege Universitesi Kampusu Ege Teknopark, Erzene Mah., Ankara Cad. No: 309, 35100 Bornova, Izmir, Turkey

[3] Electrical and Energy Department, Ostim Vocational School, Gazi University, Ostim Mah., Cevat Dundar Cad. No: 19, Ostim, Ankara, Turkey

[4] Electrical and Electronics Engineering Department, Karabuk University, 100. Yil Mh., Demir Celik Kampusu, Merkez, Karabuk, Turkey

1 Introduction

The place of wind energy, which is 3% in global electricity market today, is expected to rise up to 6% in 2023 [1]. In this respect, wind energy is a concept that has been extensively studied in all over the world, and research development activities related to these issues have increased in the last few years.

In the world, several wind turbine structures have been developed and produced to maximize the annual energy capture capacity, minimize costs, improve power quality and ensure consistent dynamic response [2]. DC excitation generators, induction and permanent magnet synchronous generators (PMSGs) are typically used wind turbine concepts [3]. In order to improve the reliability and efficiency of wind turbines, direct drive permanent magnet synchronous generators took the place of doubly-fed induction generators (DFIGs) which have been commonly used until now because of the fact that DFIGs brought some disadvantages related to wind turbine structures [2, 4, 5]. In [6], a comprehensive comparison has been presented where PMSGs have become

more advantageous than induction generators in wind energy conversion applications due to features such as high power factor, high efficiency and low installation and maintenance costs [7].

Permanent magnet electrical machines had been using in some special applications until the last 10 years. But then, the advances in electronic technology and permanent magnet materials [8] in recent years brought their usage areas into military, electric vehicle and wind energy applications. PMSGs particularly have an important position in low wind speed applications [3, 9, 10]. In the literature, several studies were carried out related to permanent magnet synchronous machines having different rotor structures as inner-rotor [11–13] and outer-rotor [14–16]. The number of poles in a normally designed inner-rotor PMSG is low. In order to achieve normal frequency at low wind speed, higher number of poles and accordingly higher diameter for the machine are required. An optimum solution should be offered considering factors such as power density, cost and efficiency for an economical design [14]. It is indicated that inner-rotor structure offers a unique solution to meet all these requirements.

The need for the systems such as generator/alternator, which are used in electricity production from wind turbine, and wind turbine is increasing together with the wind energy solutions. The importance of the design and manufacture of these systems is increasing every day as well. Currently, the electrical machine design processes are becoming more complicated [17]. As shown in Fig. 1, the design process of the generator is terminated after passing the electromagnetic, structural and thermal design and analysis stages.

There are important and independent parameters in the design of electrical machines. In the case that an optimal solution is intended in the design, the solution becomes extremely complex unless some of these independent parameters are properly constrained [18]. Many of these independent parameters rarely change. So, these parameters are assumed as constants to simplify the solution [19, 20].

Due to the issues mentioned above, the verification of the design and the need to offer optimal solution cause the process to be more complex, costly and time-consuming. Large domain and high sophistication appearing in these designs increase the need for simulation and analysis tool. Therefore, finite element method (FEM) model analyzed together with dynamic simulation seems appropriate to meet the needs of this complex structure [17].

The coupled field-circuit model (co-simulation) has been used for the analysis of electrical machines in the literature [21–23]. In [19], two basic co-simulation (direct coupling and indirect coupling) approaches are presented. But, in these studies, a detailed analysis has not been submitted for different wind speeds and different network conditions. This study enables the observation of the parameters and comprehensive dynamic performance of 4-kW inner-rotor

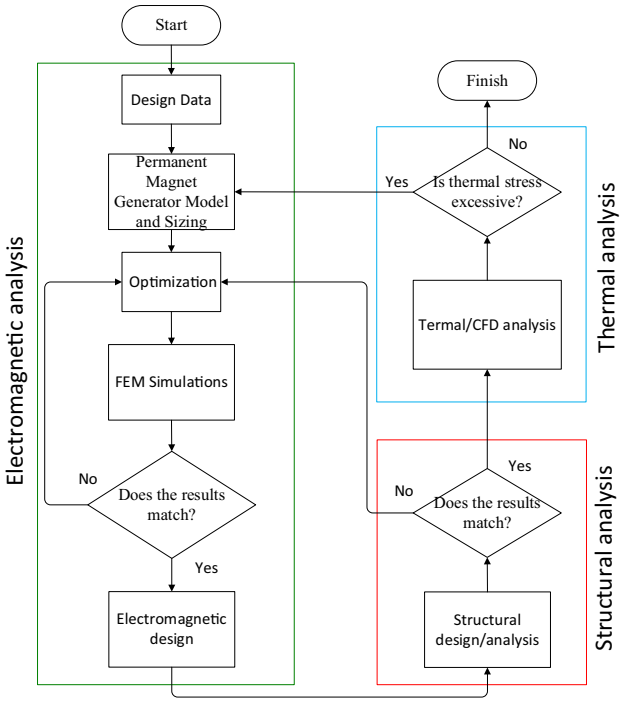

Fig. 1 Flowchart of generator design process

PMSG supplying different loads at variable speeds by using time-stepping, coupled field-circuit and two-dimensional (2D) FEM model. Furthermore, the obtained simulation results were verified by experimental results in which the wind turbine generator is acting as a voltage supplier for a water heating system.

2 System design

Wind turbine generators are primarily employed for electricity generation. Generated power can be stored in a system consisting of batteries or connected to the mains supply choosing an appropriate grid tie inverter. In case of strong winds or while the batteries are totally charged, employed wind turbine generator may supply more current than the batteries can go with. Therefore, a dump load is often used to divert the extra energy to heat water so it is not wasted. Besides, a protection method for the generator is put forward in that way. In the proposed study, the wind turbine is directly connected to a water heating system which is basically a resistive load block. Generally, it is not possible to connect a water heating element directly to the output from a wind turbine generator. The voltages generated by a wind turbine are typically far in excess of their nominal voltage rating/over-voltage values are often recorded in heavy winds. These high voltages would rapidly burn out the heating element when you need it most. So, a small battery should be

used as a buffer between generator output and the heating element in order to avoid heating element from fluctuating over-voltages. The system is designed by taking this significant case into account. Typically, the voltage or current waveform is not so important for a water heating system since the power generated will be directly used to heat water. But, in the study, because of the fact that the system can be used for any off-grid application as shown in Fig. 2, the voltage waveforms are processed for ideal outputs. So, first of all, the voltage generated by different generator speeds (simulated different wind speeds) is directly applied to load group.

Figure 2 shows the structure of the proposed model which consists of a 2D FEM model of in-running rotor-type PMSG and a circuit model divided two three parts. While one part has a measurement, other part shows connection to off-grid side.

Table 1 Given data for PMSG

Parameter	Data
Rated output power (kW)	4
Rated power factor	0.98
Rated voltage (V)	400
Number of poles	24
Frequency (Hz)	50
Rated speed (rpm)	250
Number of phases	3
Material properties	
Stator case	Aluminum 7075
Stator core	M330-50A
Rotor steel	ST52
Magnet type	N40SH (nickel-plated)
Remanence B_r (T)	1.28
Relative permeability μ_{rec}	1.05
Coercive force H_c (kA/m)	989

2.1 General considerations for PMSG

The design work on PMSG was carried out according to the general data given in Table 1. In order to provide a 50-Hz operating frequency at nominal speed, the number of poles of the machine is calculated accordingly.

In electrical machine design, there are two basic design concepts as output coefficient (machine constant) [10, 12, 18, 24] and rotor tangential stress [12]. The rotor dimensions can be identified by using appropriate tangential stress on rotor surface. If rotor radius is r_r, rotor stack length is L', the rotor surface facing the air gap is S_r, rotor diameter is D_r and average tangential stress on rotor surface is $\sigma_{F\tan}$, the torque produced by the rotor can be simply expressed as [19, 25];

$$T = \sigma_{F\tan} r_r S_r = \sigma_{F\tan} \pi \left(\frac{D_r^2}{2} \right) L' = 2\sigma_{F\tan} V_r \tag{1}$$

The exact rotor volume V_r to produce a certain rotor torque is simply calculated with this equation. The

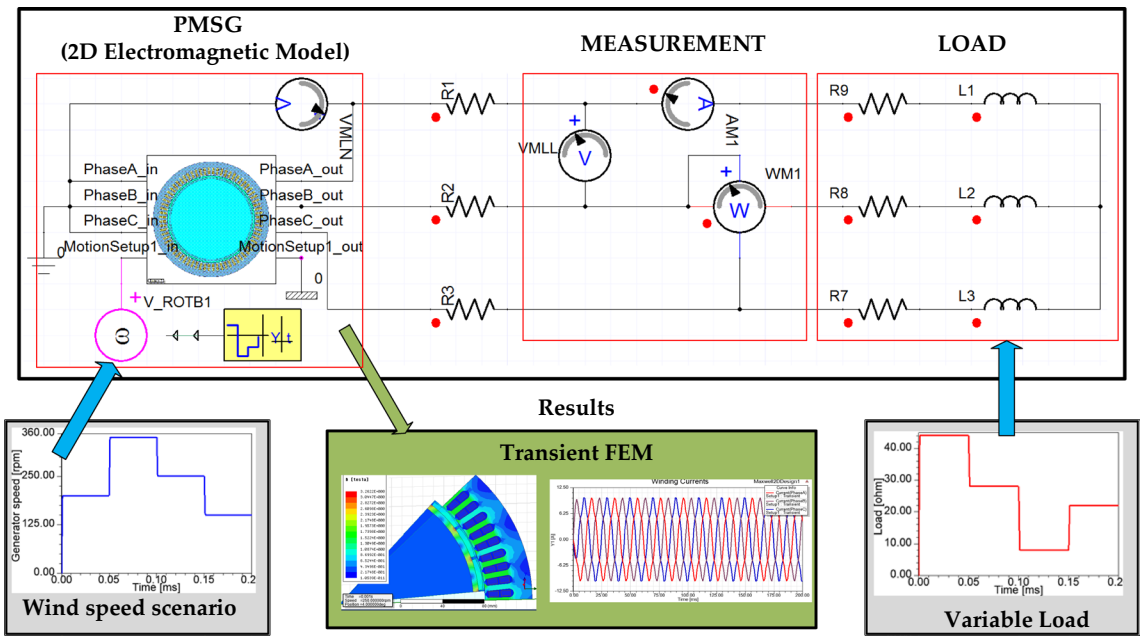

Fig. 2 Structure of field-circuit model including co-simulation

machine coefficient C of a well-designed electrical machine refers to the rotor volume of the machine and apparent air-gap electromagnetic power S_g. The other constant affecting this power is $D_{is}^2 L$ [12, 18, 24]. Fundamental machine design starts with the main dimensions of the machine, the stator bore diameter or the air-gap diameter (D_{is}) and the selection of equivalent core/stack length (L'). These main dimensions can be estimated on the basis of the output coefficient and the stack length-to-pole pitch ratio λ as follows.

The apparent electromagnetic power from [12] is:

$$S_g = mE_f I_a = 0.5\pi^2 k_w D_{is}^2 L' n_s B_g A \tag{2}$$

where $n_s = 60\,f/p$ is the synchronous speed, k_w is the stator winding factor, m is phase number, B_g is the average value of air-gap magnetic flux density of NdFeB PM synchronous machine which is called as specific magnetic loading ranging from 0.65 to 0.85 T [24] and A is the linear current density which is called as specific electric loading ranging from 35 to 65 kA/m [19]. It is important to know the ranges of these significant parameters prior to design calculations. According to these assumptions, the output power and output coefficient of the machine are calculated, respectively;

$$P_{out} = mV_a I_a \eta \cos\phi = \frac{1}{\varepsilon} S_g \eta \cos\phi \tag{3}$$

$$C = \frac{P_{out}\varepsilon}{D_{is}^2 L' n_s} = 0.5\pi^2 k_w B_g A \eta \cos\phi \tag{4}$$

The $D_{is}^2 L$ output coefficient may be calculated from machine constant equation:

$$D_{is}^2 L = \frac{P_{out}\varepsilon}{C n_s} \tag{5}$$

The other step in the calculations is the separation of this multiplication as D_{is} and L components. There is not a standard value for λ, which is the stack length-to-pole pitch ratio in machine applications. Alternatively, in [19], an equation of the stack length-to-pole pitch ratio was given for synchronous machines as a function of pole pair as follows:

$$\lambda = \frac{L'}{D_{is}} \approx \frac{\pi}{4}\sqrt{p} \tag{6}$$

In this paper, once the design parameters and dimensions of the permanent magnet synchronous generator are determined from the results of the analytical design study, the multiobjective optimization approach is used to achieve optimum generator design. This approach is usually preferred choosing the best solution considering different objectives. Usually, there is no single best solution in electrical machine design, but a set of solutions are equally well. So the general form of the multiobjective optimization problem can be expressed mathematically as [26]:

$$\text{GoalFunction} = \begin{Bmatrix} \max/\min.\, y_j = f(x),\ j = 1,2,3,\ldots \\ y = P_{loss},\ \text{efficiency},\ V_{out},\ T_{cog} \\ x_{bound}^{low} \le x_i \le x_{bound}^{upper},\ i = 1,2,3,\ldots \\ x = L,\ b_{s0},\ h_m,\ \tau,\ \text{skew} \end{Bmatrix} \tag{7}$$

The multiobjective optimization problems include output characteristics of machine such as load line voltage, output power, cogging torque and efficiency. The parameters

- slot opening: 1 mm $\le b_{so} \le$ 3 mm, ++0.1 mm
- pole pitch/magnet pitch ratio: $0.5 \le \tau \le 1$, ++0.02
- the height of magnet: 3 mm $\le h_m \le$ 10 mm, ++0.2 mm
- the stack length: 70 mm $\le L \le$ 115 mm, ++5 mm
- skew the rotor magnets: $0 \le$ skew ≤ 1, ++0.2

have been optimized to obtain the generator with the appropriate output values that meet the requirements in this paper. The design parameters and dimensions of the permanent magnet synchronous generator determined as a result of analytical design and optimization study are given in Table 2 comparatively.

After optimization, the generator efficiency is about 93%. This value is very satisfactory for applications of this scale. When the length of the body is reduced, the efficiency increases to approximately 95%. However, while lower body length increases the efficiency, it causes the line voltage and output power to fall below the desired value. PMSG-based variable speed wind turbine applications require a DC–AC conversion process. Line voltage and output power have been increased by taking into account the losses in this transformation.

Table 2 Comparison of initial and optimum values of the generator

Parameter	Initial	Optimized	Improvement
Line voltage (V)	389	421	+32
Phase current (A)	6.22	6.73	+0.51
Specific electric loading (A/m)	27,508	30,867	−3359
Current density (A/mm^2)	2.17	3.54	−1.37
Total loss (W)	208	363	−155
Rated power (kW)	4.17	4.88	+0.71
Efficiency (%)	95.25	93.07	−2.18%
Power factor	0.94	0.98	+0.04
Rated torque (Nm)	167.4	200.5	+33.1
Short circuit current (A)	33.73	26.9	+6.83
Cogging torque (Nm)	17.89	0	+17.89
THD% (back emf)	19.56	1.26	+18.8

Furthermore, the parameter of cogging torque becomes greatly more of an issue in especially low-speed wind turbine applications and electric power steering systems [27, 28]. Reducing the cogging torque helps to reduce torque ripple, mechanical vibration and acoustic noise [29]. Herewith, we provide a smooth electromagnetic torque [30–32]. Therefore, the cogging torque is reduced using the multi-objective parameters given in (7). For instance, in order to reduce cogging torque, rotor magnets are skewed by one slot, the magnet thickness h_m is set as 5 mm and slot opening b_{so} is set as 2.2 mm.

Once employing finite element method on designed machine and applying the coupled circuit analysis, it would be better to give a simplified 3D visualization related to the final design as shown in Fig. 3.

The stator windings of the generator consist of 1.1-mm conductor and 2 layers of 672 turns (per phase). The current density obtained is approximately 3.54 A/mm^2. This value is also an acceptable density value. It is recommended to keep the current density between 3.5 and 8 A/mm^2 depending on the power rate in the design of electrical machines. In addition, high energy density of Nd–Fe–B materials allows the use of smaller magnets. However, Nd–Fe–B magnets are used for low volume and low weight in this article. The supplied magnets, the pictures of the rotor yoke and machined shaft are given in Fig. 4.

3 2D FEM model of PMSG

Some methods are used to analyze the magnetic field and performance of electrical machines which are consisting of two- and three-dimensional analyses, basically the most preferred methods. A time-stepping, co-simulation is developed using a 2D FE package in order to present the analysis and performance of a PMSG supplying a different load condition in [23]. A new two-dimensional magnetostatic FEM is proposed to estimate the steady-state performance of the PMSG in [33]. A magnetostatic model of a PMSG is important because it can then be used as a starting point in a transient analysis or evaluation of a new generator design [33].

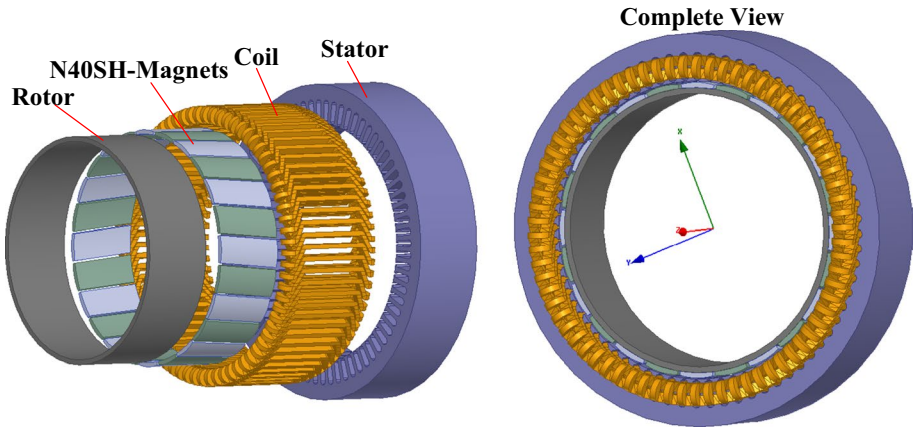

Fig. 3 3D model of PMSG

Fig. 4 Manufactured parts of PMSG

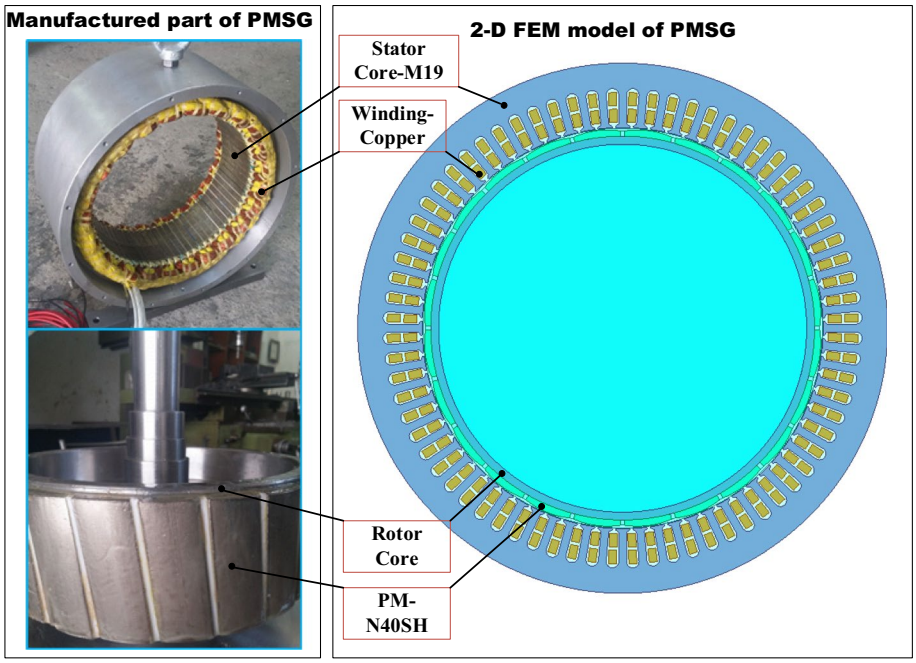

Fig. 5 2D FEM model for electromagnetic performance assessments

In the case that the number of poles of the machine is high (as in the application of which 2D electromagnetic details are given in Fig. 5), 2D analytical solutions and FEM provide highly accurate solutions for the magnetic field distribution and machine performance. In this paper, 2D FEM transient solver was chosen to analyze the magnetic fields, energy, force/torque, power loss, core loss, speed, and flux of a model at various time steps. There are some limitations and assumptions for 2D FEM transient solver as follows [34]:

- Magnetic field solution is proportional to changing air gap/pole arc ratio and radius of the selected cylindrical cutting plane;
- Mutual and leakage fluxes in the end-winding cannot be taken into account;
- It is not used for the analysis of the materials with different cross sections;
- Rotational motion can be cylindrical or non-cylindrical.

Most of the physical issues in electrical energy systems can be described by quasi-static phenomena [35]. An electromagnetic problem can be described with the distribution of the magnetic field strength when given a source input (current density or voltage) as follows:

$$J = \sigma(\vec{E} + v \times \vec{B}) \tag{8}$$

$$\vec{E} = \mu_0(\vec{H} + \vec{M}) \tag{9}$$

where J is the electric current density, $\vec{B}$ is the magnetic flux density vector, σ is the electrical conductivity, μ_0 is the magnetic permeability of free space, v is the velocity of the material with respect to a given reference frame, $\vec{E}$ is the electric field intensity and $\vec{M}$ is the magnetization vector. The magnetic vector potential $\vec{A}$ and the electric scalar potential Φ are commonly used potentials to solve electromagnetic problems in which two-dimensional model is based on the assumption that the magnetic vector potential and current density have only z-axis components and their values are determined in the xy-plane and then nonlinear time-varying moving electromagnetic field solved by FEM. The 2D XY problem of the electromagnetic field is described as follows [33, 36]:

$$\frac{1}{\mu_0}\nabla \times (\nabla \times \vec{A}) - \nabla \times \vec{M} = -\sigma \nabla \Phi - \sigma \frac{\mathrm{d}\vec{A}}{\mathrm{d}t} + \sigma v \times (\nabla \times \vec{A}) \tag{10}$$

The first term on the right-hand side, J_s, is the source current density due to differences in electric potential, and second term on the right-hand side J_e is the induced eddy current density due to time-varying magnetic fields. Also, the 2D XY problem can be reduced to scalar form, and the magnetic vector potential $\vec{A}$ is reduced to the z-axis scalar A_Z [14, 22, 36]:

$$\sigma \frac{\mathrm{d}\vec{A}_Z}{\mathrm{d}t} - \frac{1}{\mu_0}\nabla^2 A_Z = -\sigma \nabla \Phi + \nabla \times \vec{M} \tag{11}$$

In relation to that, in the case that the current flowing in the stator winding is modeled as stranded coils; the current densities for stranded coils are given by [34]:

$$J_s = -\frac{1}{\mu_0}\nabla^2 A_Z = \frac{n_c}{S_c} \tag{12}$$

where n_c is the number of turns, S_c is the cross-sectional area of the coil, $i(t)$ is the current per turn.

In the study carried out, ANSYS Maxwell 2D package is used in which finite element analysis is employed to prove the correctness of the values calculated numerically. Magnetic analysis instead of quantitative techniques is preferred to determine the structure of designed prototype generator. Magnetic flux density distribution in the air gap and the stator yoke is presented in Fig. 6 as a result of derived simulations.

In order to see the flux densities on the machine, the flux density distribution in the whole section of the machine (Fig. 6a) has been obtained with a 10° rotor rotation. Here, the rotor yoke density is around 0.9 T in the center of the pole spring and 2.06 T for the opposite sides of the rotor. Also, the flux density of the magnet is around 0.83 T. Magnet flux density is an important parameter for demagnetization analysis. The average flux density value on the entire surface is 1.3 T, while the air-gap flux density is around 0.8–1 T. In addition, stator teeth flux density is 1.5 T. As the saturation point of silicon steel sheet used was 1.7 T, the sheet did not face saturation. Thus, the hysteresis losses of the machine will be very low. Figure 6b shows the magnetic flux and flux path formed in magnets. The leakage of the magnet and the air gap through the slots has not been observed. Also, the amount of leakage flux between adjacent magnets in the opposite direction is not large.

3.1 Circuit coupling method

In today's research and development processes, the simulation of dynamic systems allows predictions and concept decisions related to the final product to be made at an early stage. This not only involves the modeling, simulation and testing of individual structural components or modules, but also requires the interplay of a large number of functions (with simulation models and hardware components from various domains) to build up the full system.

The term "co-simulation" refers to a simulation approach where the components of modern mechatronic systems are interconnected in a suitable way. Therefore, the complex interactions between these subsystems from different development environments are taken into account. The coupling of existing (specific) simulation programs (and the models implemented therein) from different areas of expertise represents a promising approach for the simulation of the overall system.

There are two basic approaches to couple electromagnetic field with circuit simulation. One is the direct coupling approach where Maxwell 2D and 3D FEA models can

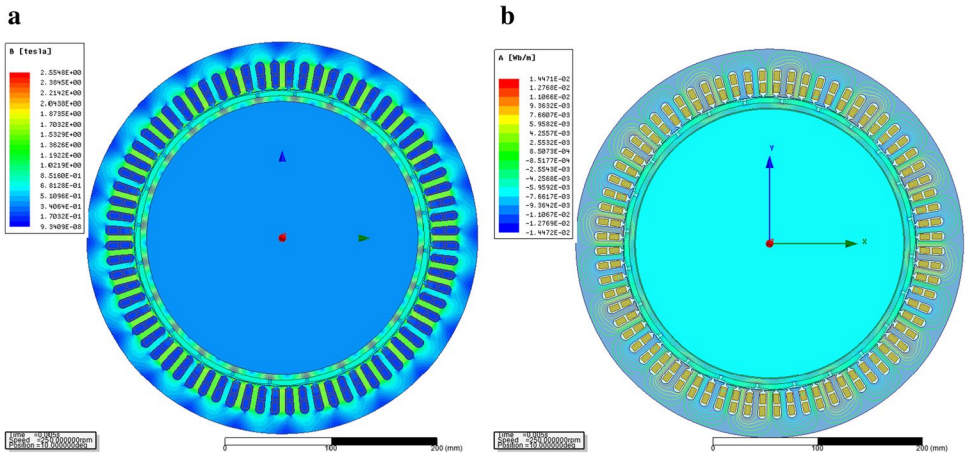

Fig. 6 Field distribution on the entire surface of the PMSG. **a** Magnetic flux density and **b** active flux paths

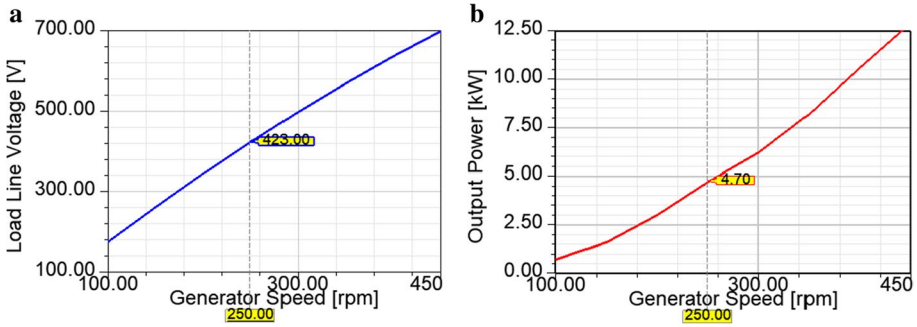

Fig. 7 Generator performance for variable speed and constant load: **a** Load line voltage and **b** output power

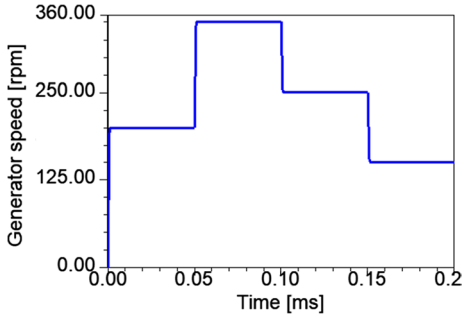

Fig. 8 Wind speed-dependent generator speed regime

be solved simultaneously with a transient circuit system simulation model [21–23, 37]. Namely, a direct coupling co-simulation is achieved by a data exchange between transient solvers during each time step. It offers a good solution if eddy effects are important for the simulation, and the system either has nonlinear materials or motion. The second approach is co-simulation by indirect coupling where the electromagnetic field and circuit simulator are treated as separate systems in a step-by-step process with respect to time including values for end time, minimum time step and maximum time step [21].

The main idea behind conducting a coupled electromagnetic analysis is that the results obtained via simulations will provide comprehensive information and data related to the behavior of the machine in different conditions. Moreover, it is possible to confirm the accuracy and sensitivity of the analytical calculations. The circuit presented in Fig. 2 is giving the details of co-simulation model used in analysis.

Related model is used to carry out simulations in two steps. In the first step, the generator was operated for a time period of 100 ms at varying speed rates ranging from 100 to 450 rpm (100–150–200–250–300–350–400–450 rpm) for constant load condition ($R_L = 36\ \Omega$). For each condition, the obtained results are given in Fig. 7. From the outcomes, it is noted that both load line voltage and the output power for the same load go up with the increase in speed (wind speed in that case).

The variation of pure generator voltages and currents, output power and core loss are presented, are shown in Fig. 9 for a time period of 200 ms at operating wind speed regime is presented in Fig. 8.

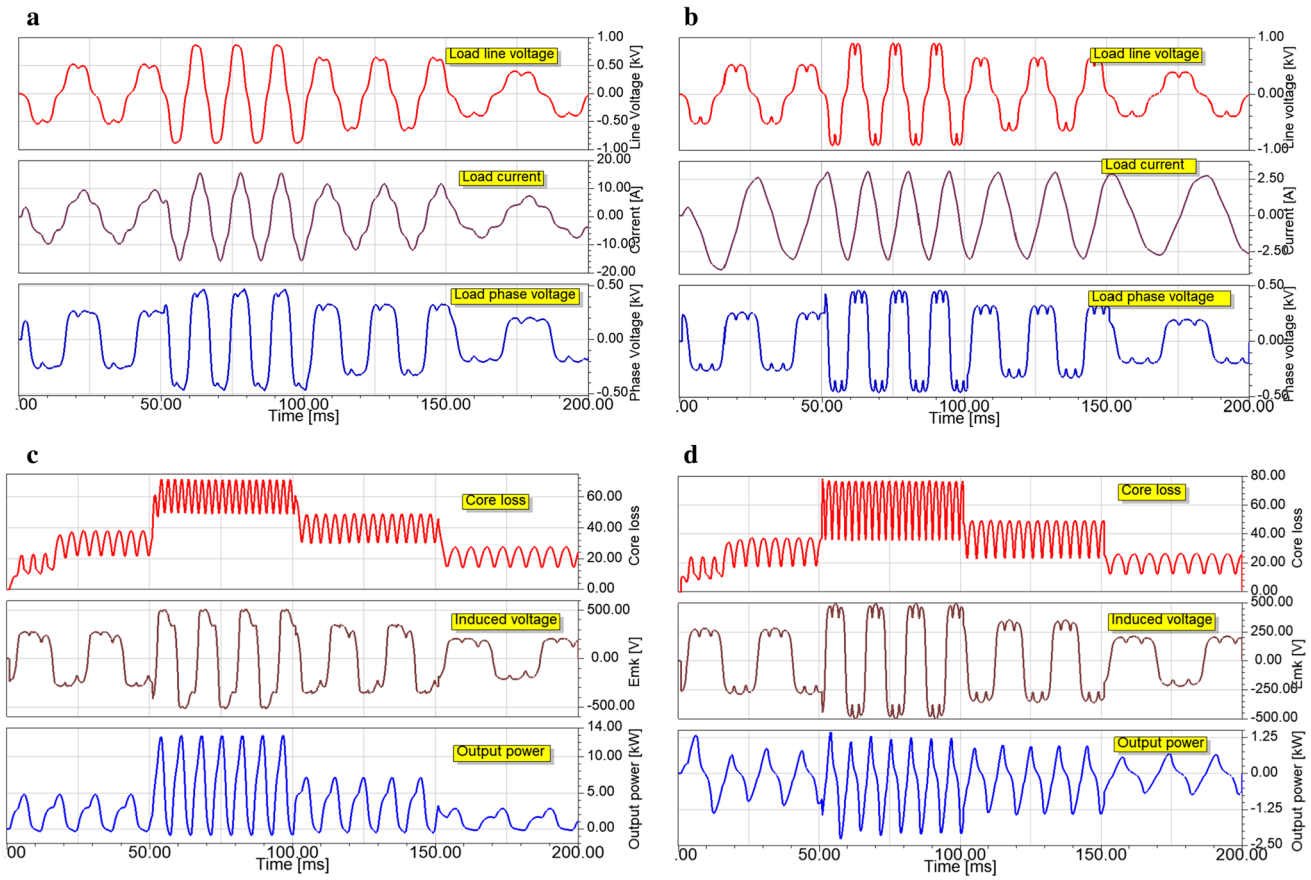

Fig. 9 Generator performance for variable speed and constant load. **a** Load-side measurements (ohmic load), **b** load-side measurements (inductive load), **c** generator-side measurements (ohmic load), **d** generator-side measurements (inductive load)

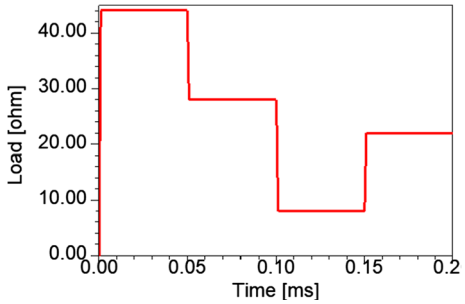

Fig. 10 Variable load conditions (ohmic)

The dynamic response of the generator is particularly good at the points where the speed value increases and decreases unexpectedly. Figure 9c, d shows that iron loss increases when speed increases. In addition, the amplitude of the 3rd and 5th harmonic components was high, causing distortions in the waveform. This negative case can be eliminated by the combination of fractional slot/pole combination. The waveforms of the comparative output voltages indicate that the inductive load increases the distortion in the basic waveforms.

In the second step, the variable load conditions at the rated speed for the output characteristic of the machine are defined as given in Fig. 10 as an operating scenario at a given time interval. PMSG, thus a closer look to real-time operating condition, is taken into consideration. The related results are demonstrated in Fig. 11.

It is possible to indicate that the generator is giving a smooth reaction, especially where the load value is unexpectedly increased. Some fluctuations have been observed due to sudden changes in torque. The load-side analysis shows that the generator is very strong to provide the appropriate line voltage for the load when the load case has been changed (Fig. 11a). On the other hand, it is understood from the waveforms that the harmonic effect is less due to low resistance value defined between 100 and 150 ms. These transient solutions were obtained within 100 µs steps between 0 and 200 ms. More accurate results can be obtained if these time steps are chosen smaller.

So, the trend of voltage, current and power as a generator performance shows a good agreement, which can be easily preferred for an off-grid operating system next to water heating purpose.

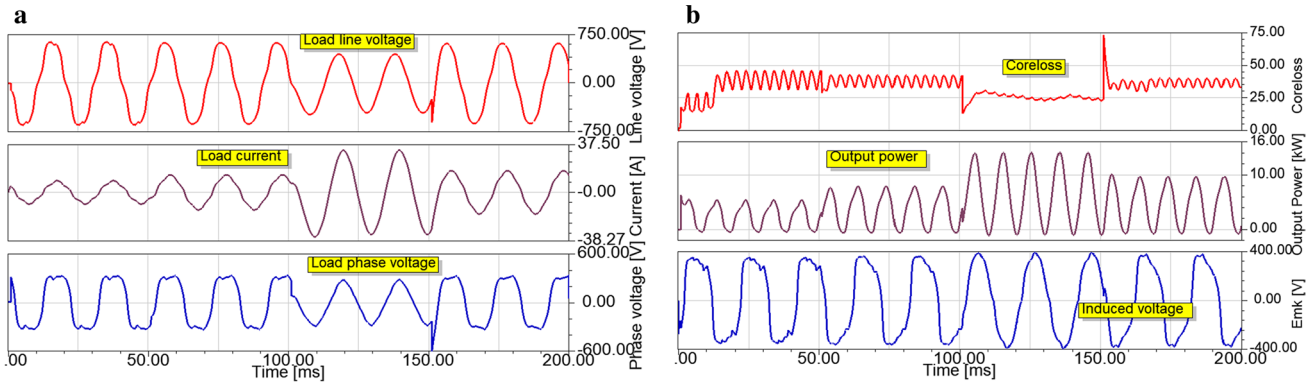

Fig. 11 Generator performance for constant speed and variable load. **a** Load-side measurements and **b** generator-side measurements

Fig. 12 Test setup

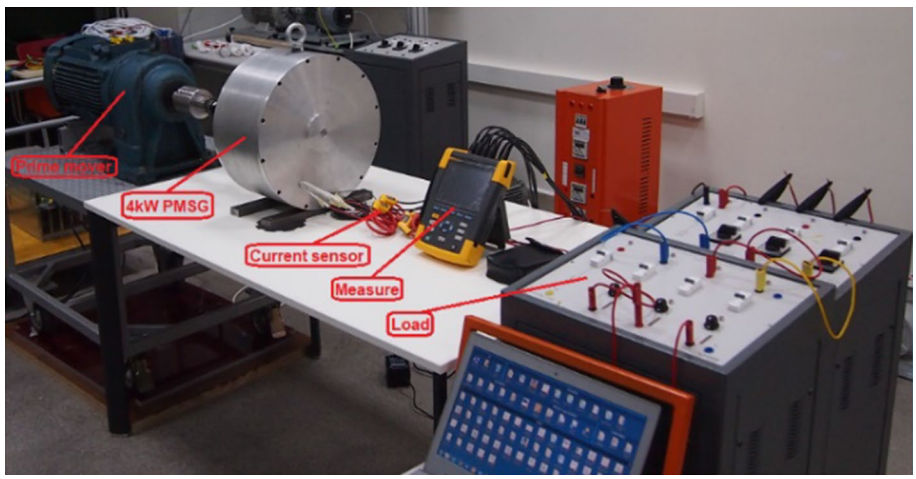

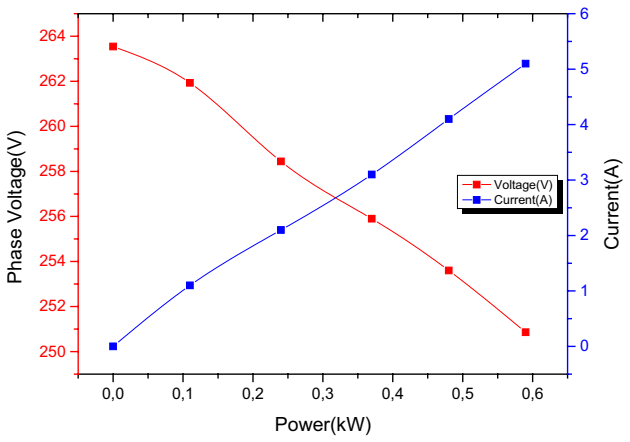

Fig. 13 Output characteristic of PMSG

Since the load rate and rotation speed of the designed prototype are varied for each of conditions, it gives us a comprehensive aspect regarding the dynamic response of the generator.

4 Experimental study

To verify the electromagnetic design and co-simulation results, a prototype for the experimental tests was manufactured and tested as shown in Fig. 12. This test setup comprises a 4-kW PMSG prototype, measurement devices, variable load system, variable speed driver and induction motor for ensuring rotational speed of PMSG which is simulating wind speed in that application.

To obtain the output characteristics of PMSG in different load conditions according to rated speed (250 rpm), the rates of supplied resistance loads are varied accordingly and the illustration shown in Fig. 13 is derived, in which power versus phase voltage and current variation is presented. As the output power of the generator is increased (loaded), phase voltage is decreased and current is increased as shown in the figure.

In addition, the chart related to terminal voltage, current and power values obtained at rated speed and rated load (ohmic and inductive) is given in Fig. 14. When the terminal voltage chart is examined, it is seen that the inductive load increases the distortion of sine wave compared to the ohmic load (Fig. 14a, d). It should be noted that the inductive load increases the 5th harmonic as shown in Fig. 14b, e. And also active power is reduced at inductive load (Fig. 14f). This explains the effect of nonlinear loads on harmonics.

4.1 Verification

In this section, in order to verify the agreement of proposed simulation model, equivalent circuit model and experimental some studies are carried out. Furthermore, experimental, simulation and analytical calculation results obtained for

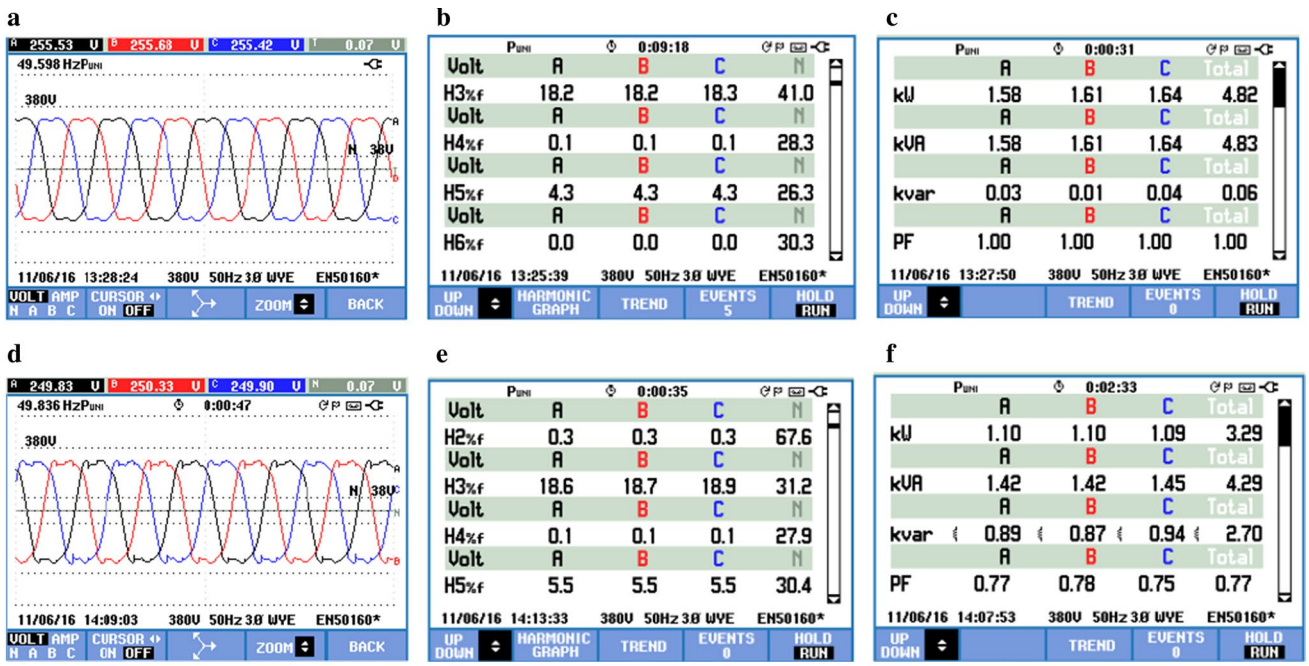

Fig. 14 Results of measurements for constant speed and rated load (R–R_L). **a** Phase voltage (R), **b** harmonic content (R), **c** power values (R), **d** phase voltage (R_L), **e** harmonic content (R_L), **f** power values (R_L)

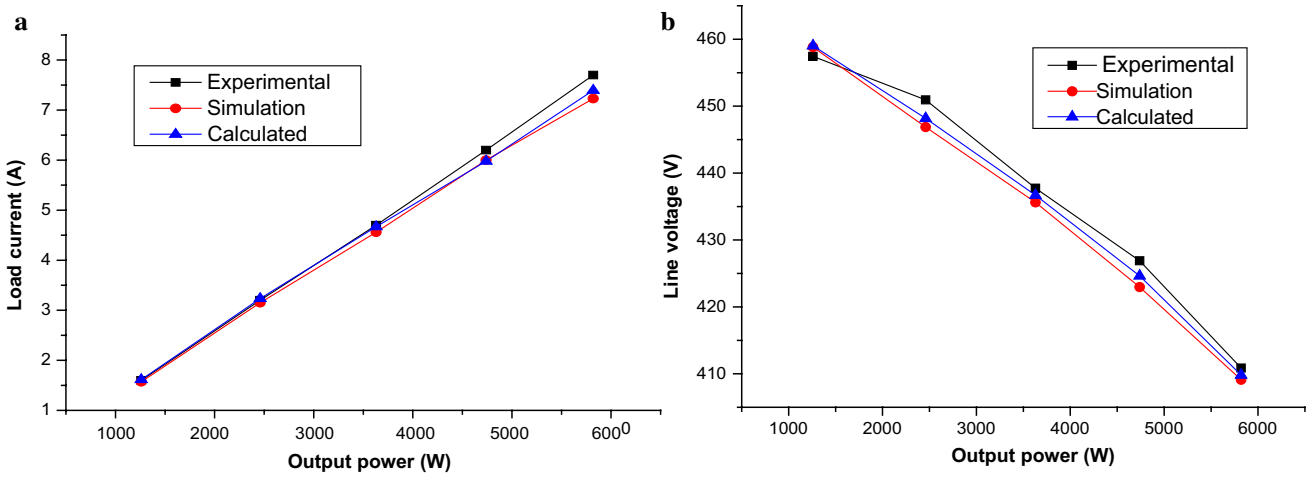

Fig. 15 Output characteristic for rated speed and variable load (R). **a** Load current, **b** load line voltage

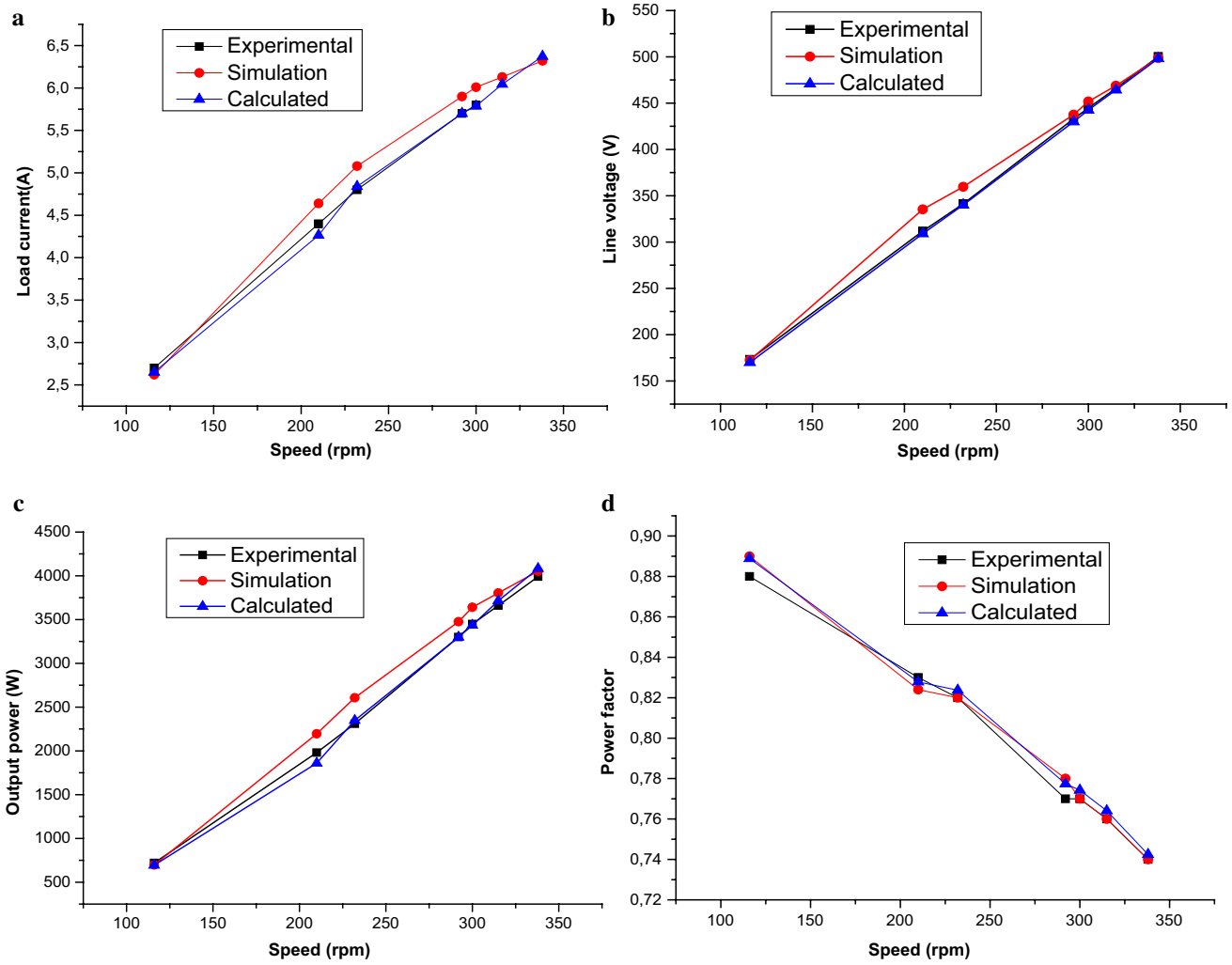

Fig. 16 Output characteristic for variable speed and rated load (R–L). **a** Load current, **b** load line voltage, **c** output power, **d** power factor

different operating conditions of the generator are presented comparatively. Variation of load current and line voltage relating to varying ohmic loads and rated speeds is given in Fig. 15.

Furthermore, the generator output characteristic relating to varying speeds and rated loads (*R–L*) is given in Fig. 16. According to the results obtained from Fig. 15, simulation results are in good agreement with experimental studies, indicating that the generator dynamic performance can be precisely estimated by using co-simulation.

5 Conclusion

In that study, the dynamic analysis of a three-phase surface mounted PMSG has been presented. A direct co-simulation approach has been applied and a 2D FEM is used for the electromagnetic field solution. Following simulation studies, 4-kW PMSG has been successfully designed and prototyped. For a water heating system in which only resistor block has been used as a load. It should be noted that this system is not only suitable for water heating system but also useful for any off-grid turbine application. Moreover, the similar results between the co-simulation and experimental studies at the same load characteristics have been obtained posterior to experimental studies. To make a comparison between simulation and experimental works for rated speed and variable load (ohmic) conditions, it can be stated that the preliminary measurement outcomes indicate that the generated load line voltage is about 5% higher than expected from two-dimensional co-simulations. In other words, the generated voltage resulted higher than predicted. Besides, load current is about 3% higher than expected. These differences between experimental results and simulations are most likely caused by the simulations carried out with a 2D simulation method. If 3D method had been used, a better result would be reached due to the fact that 3D simulations are taking more losses and transients into account during simulation process.

In order to summarize, co-simulation approach is an effective method to demonstrate compliance with real load conditions prior to the manufacture of the designed machine. In addition, in this study, it can be easily stated that permanent magnet synchronous generators or alternators are pure sinusoidal power sources for grids or power conversion tools in off-grid systems.

Acknowledgements This work was supported by the Scientific and Technological Research Council of Turkey (TUBITAK) under Grant EEEAG-113E782.

References

1. IEA, International energy agency (2018) Renewables 2018. https://www.iea.org. Accessed 8 Oct 2018
2. Cheng M, Zhu Y (2014) The state of the art of wind energy conversion systems and technologies: a review. Energy Convers Manag 88:332–347
3. Guo Z, Chang L (2005) FEM study on permanent magnet synchronous generators for small wind turbines. In: Canadian conference on electrical and computer engineering, 2005. IEEE, pp 641–644
4. Hemeida AM, Farag WA, Mahgoub OA (2011) Modeling and control of direct driven PMSG for ultra large wind turbines. World Acad Sci 59:918–924
5. Bhende CN, Mishra S, Malla SG (2011) Permanent magnet synchronous generator-based standalone wind energy supply system. IEEE Trans Sustain Energy 2(4):361–373
6. Polinder H, Van Der Pijl FFA, De Vilder GJ, Tavner PJ (2006) Comparison of direct-drive and geared generator concepts for wind turbines. IEEE Trans Energy Convers 21(3):725–733
7. Erken F, Öksüztepe E, Kürüm H (2016) Online adaptive decision fusion based torque ripple reduction in permanent magnet synchronous motor. IET Electr Power Appl 10(3):189–196
8. Kurt E, Gör H, Demirtaş M (2014) Theoretical and experimental analyses of a single phase permanent magnet generator (PMG) with multiple cores having axial and radial directed fluxes. Energy Convers Manag 77:163–172
9. Grant J (1951) Diphtheria in gateshead, 1936–46. Public Health 65(C):3–5
10. Uygun D, Ocak C, Cetinceviz Y, Demir E, Gungor Y (2012) CAD-based design, analysis and experimental verification of an out-runner permanent magnet synchronous generator for small scale wind turbines. In: 2012 11th international conference environment electrical engineering EEEIC 2012—conference proceedings, pp 179–183
11. Wang H, Fan J (2010) Analysis and performance evaluation of compound permanent magnet generator with controllable airgap flux. In: Digest 2010 14th biennial IEEE conference on electromagnetic field computation CEFC 2010, vol 5, pp 684–690
12. Tapia JA, Pyrhönen J, Puranen J, Lindh P, Nyman S (2013) Optimal design of large permanent magnet synchronous generators. IEEE Trans Magn 49(1):642–650
13. Wang T, Wang Q (2012) Optimization design of a permanent magnet synchronous generator for a potential energy recovery system. IEEE Trans Energy Convers 27(4):856–863
14. Tomczuk B, Schroder G, Waindok A (2000) Design and finite-element analysis of an outer-rotor permanent-magnet generator for directly coupled wind turbines. IEEE Trans Magn 43(7):3802–3809
15. Potgieter JHJ, Kamper MJ (2012) Torque and voltage quality in design optimization of low-cost non-overlap single layer winding permanent magnet wind generator. IEEE Trans Ind Electron 59(5):2147–2156
16. Eriksson S, Bernhoff H, Bergkvist M (2012) Design of a unique direct driven PM generator adapted for a telecom tower wind turbine. Renew Energy 44:453–456
17. Makolo P (2013) Wind generator co-simulation with fault case analysis. Master of Science Thesis, Chalmers University of Technology, Department of Energy and Environment, pp 1–75
18. Mihai AM, Benelghali S, Simion A, Outbib R, Livadaru L (2012) Design and FEM analysis of five-phase permanent magnet generators for gearless small-scale wind turbines. In: Proceedings—2012 20th international conference on electrical machines ICEM 2012, pp 150–156

19. Pyrhonen J, Jokinen T, Hrabovcov V (2008) Design of rotating electrical. Wiley, Hoboken
20. Kilk A, Kudrjavtsev O (2012) Study and verification of a slow speed PM generator with outer rotor for small scale wind turbines. In: PQ 2012 8th international conference—2012 electric power quality and supply reliability conference proceedings, 2012, pp 19–24
21. Zhou P, Lin D, Fu WN, Ionescu B, Cendes ZJ (2006) A general cosimulation approach for coupled field-circuit problems. IEEE Trans Magn 42(4):1051–1054
22. Kelly MG, Newton WL, O'Gara RW (1962) Susceptibility of newborn germ-free mice to tumor induction by 3-methylcholanthrene. Cancer Res 23:978–982
23. Chan TF, Wang W, Lai LL (2010) Analysis and performance of a permanent-magnet synchronous generator supplying an isolated load. IET Electr Power Appl 4(3):169
24. Huang S, Luo J, Leonardi F, Lipo TA (1998) A general approach to sizing and power density equations for comparison of electrical machines. IEEE Trans Ind Appl 34(1):92–97
25. Boldea I, Nasar SA (2018) The induction machines design handbook. CRC press
26. Cetinceviz Y, Durmus Uygun HD (2017) Optimal design and verification of a PM synchronous generator for wind turbines. Int J Renew Energy Res 7(3):1324–1332
27. Kim K-S, Jung K-T, Kim J-M, Hong J-P, Kim S-I (2016) Taguchi robust optimum design for reducing the cogging torque of EPS motors considering magnetic unbalance caused by manufacturing tolerances of PM. IET Electr Power Appl 10(9):909–915
28. Gulec M, Aydin M (2013) Magnet asymmetry in reduction of cogging torque for integer slot axial flux permanent magnet motors. In: IEE proceedings—electric power applications, 2014, pp 189–198
29. Zhu X, Hua W, Wu Z (2018) Cogging torque minimisation in FSPM machines by right-angle-based tooth chamfering technique. IET Electr Power Appl 12(5):627–634
30. Ren W, Xu Q, Li Q, Zhou L (2016) Reduction of cogging torque and torque ripple in interior PM machines with asymmetrical V-type rotor design. IEEE Trans Magn 52(7):1–5
31. Jin MJ, Wang Y, Shen JX, Luk PCK, Fei WZ, Wang CF (2010) Cogging torque suppression in a permanent-magnet flux-switching integrated-starter-generator. IET Electr Power Appl 4(8):647
32. Zhu X, Hua W, Wu Z (2018) Cogging torque suppression in flux-reversal permanent magnet machines. IET Electr Power Appl 12(1):135–143
33. Gonzalez A, Hernandez C, Arjona MA (2013) Two-dimensional finite element magnetostatic model of a permanent magnet synchronous generator for predicting its steady-state performance under different loading conditions. IET Electr Power Appl 7(3):207–213
34. Chan TF, Wang W, Lai LL (2010) Performance of an axial-flux permanent magnet synchronous generator from 3-D finite-element analysis. IEEE Trans Energy Convers 25(3):669–676
35. Hofmann H (2010) Danhong thesis final
36. Zhang Y, Chau KT, Liu C (2006) A finite element-analytical method for electromagnetic field analysis of electric machines with free rotation. IEEE Trans Magn 42(10):3392–3394
37. Li XM, Yang ZX, Li YB, Chen W, Zhang LP (2017) Performance analysis of permanent magnet synchronous generators for wind energy conversion system. In: International conference on advanced mechatronic systems ICAMechS, 2017, pp 544–549